

CHAPTER 5

IMAGE CLASSIFICATION

Image classification is a complex process that may be affected by many factors. This chapter details supervised and unsupervised classification techniques. The emphasis is placed on the support vector machine classification approach and how this technique is used for improving classification accuracy.

5.1 INTRODUCTION

The amount of image data that is received from satellite is constantly increasing. For example, nearly 3 terabytes of data are being sent to Earth by NASA's satellites every day. Advances in satellite technology and computing power have enabled the study of multi-modal, multi-spectral, multi-resolution and multi-temporal data sets for applications such as urban land use monitoring and management, Geographic Information System (GIS) and mapping, environmental change, site suitability, agricultural and ecological studies. Automatic content extraction, classification and content-based retrieval have become highly desired goals for developing intelligent systems for effective and efficient processing of remotely sensed data sets.

Gong and Howarth (1992) discussed the classification of remote sensing data is a complex process and requires consideration of many factors. The user's need, scale of the study area, economic condition, and analyst's skills are important factors influencing the selection of remotely sensed data,

the design of the classification procedure and the quality of the classification results. The major steps of image classification may include image preprocessing, feature extraction, selection of training samples, selection of suitable classification approaches, post-classification processing, and accuracy assessment.

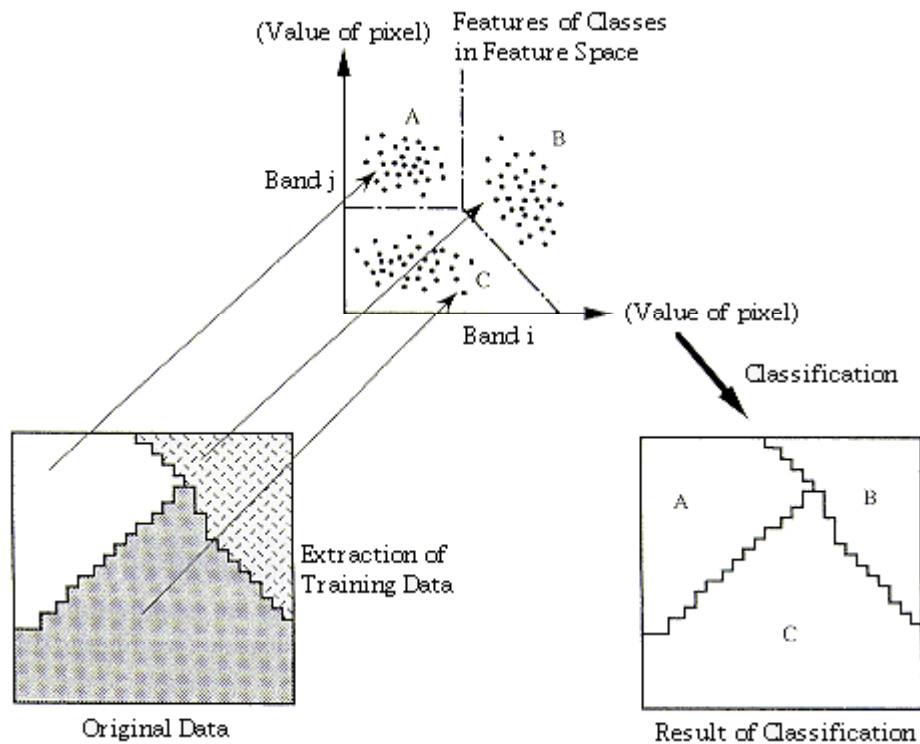


Figure 5.1 Classification of remote sensing data

Phinn et al (2000) described classification of remote sensing data is used to assign corresponding labels with respect to homogeneous characteristics of groups. The main aim of classification is to discriminate multiple objects from each other within the image. Classification will be executed on the base of spectral or spectrally defined features, such as density, texture etc., in the feature space. It can be said that classification divides the feature space into several classes based on a decision rule. Figure 5.1 shows the concept of classification of remote sensing data. In many cases, classification will be undertaken using a computer, with the use of

mathematical classification techniques. Classification will be made according to the following procedures as shown in Figure 5.2.

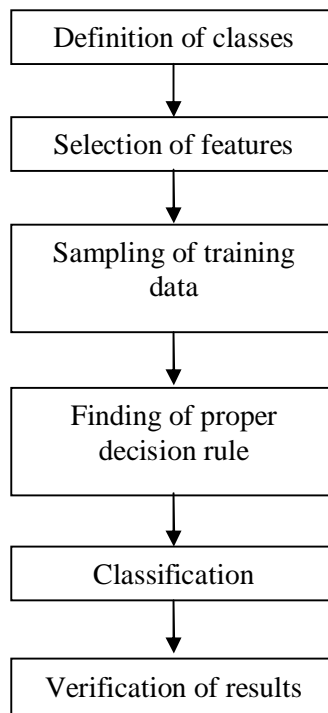


Figure 5.2 Classification procedure

Step 1: Definition of Classification Classes

Depending on the objective and the characteristics of the image data, the classification classes should be clearly defined.

Step 2: Selection of Features

Features to discriminate between the classes should be established using multi-spectral or multi-temporal characteristics, colour, textures etc.

Step 3: Sampling of Training Data

Training data should be sampled in order to determine appropriate decision rules. Classification techniques such as supervised or unsupervised learning will then be selected on the basis of the training data sets.

Step 4: Finding of proper decision rule

Various classification techniques will be compared with the training data, so that an appropriate decision rule is selected for subsequent classification.

Step 5: Classification

Depending upon the decision rule, all pixels are classified in a single class. There are two methods of pixel by pixel classification and per-field classification, with respect to segmented areas.

Step 6: Verification of Results

The classified results should be checked and verified for their accuracy and reliability.

5.2 CLASSIFICATION TECHNIQUES

The learning algorithms are broadly classified into supervised and unsupervised learning techniques. The distinction is drawn from how the learner classifies data. In supervised learning, the classes are predetermined. These classes can be conceived of as a finite set, previously arrived at by a human. In practice, a certain classes of data will be labeled with these classifications. Althausen (2002) reviewed the classes are then evaluated based on their predictive capacity in relation to measures of variance in the data itself. Some of the examples of supervised classification techniques are Back Propagation Network (BPN), Learning Vector Quantization (LVQ), Self Organizing Map (SOM), Support Vector Machine (SVM), etc.,

The basic task of unsupervised learning is to develop classification labels automatically. Unsupervised algorithms seek out similarity between

pieces of data in order to determine whether that can be characterized as forming a group. These groups are termed clusters. Unsupervised classification, often called as clustering, the system is not informed how the pixels are grouped. The task of clustering is to arrive at some grouping of the data. One of the very common of cluster analysis is K-means clustering.

5.2.1 Classification of Remote Sensing Data

Lefsky and Cohen (2003) described the intent of the classification process is to categorize all pixels in an image into one of several land cover classes, or themes. This categorized data may then be used to produce thematic maps of the land cover present in an image. Normally, multispectral data are used to perform the classification and, indeed, the spectral pattern present within the data for each pixel is used as the numerical basis for categorization. The objective of image classification is to identify and portray, as a unique gray level (or colour), the features occurring in an image in terms of the object or type of land cover these features actually represent on the ground.

5.3 THE UNSUPERVISED CLUSTERING

The unsupervised clustering is a kind of clustering which takes place with minimum input from the operator; no training sample is available and part of the feature space is achieved by identifying natural groupings of the given data. In unsupervised clustering technique, an individual pixel is compared to each cluster to see the closest pixel. Finally, a map of all pixels in the image, classified as to different clusters, each pixel is most likely to belong, is produced. This then must be interpreted by the user as to what the colour patterns may mean in terms of classes, etc. that are actually present in the real world scene; this requires some knowledge of the scene's feature or

cluster content from general experience or personal familiarity with the area imaged.

The objective here is to group multi-band spectral response patterns into clusters that are statistically separable. The cluster numbers are initially set and the total number can be varied arbitrarily. Generally, in an area within a SAR image, multiple pixels in the same cluster correspond to some ground feature or cluster so that patterns of gray levels result in a new image depicting the spatial distribution of the clusters. These levels can then be assigned to produce a cluster map. This can be done by either being adequately familiar with the major classes expected in the scene, or, where feasible, by visiting ground truth and visually correlating map patterns to their ground counterparts. Since the classes are not selected beforehand, this method is termed as unsupervised classification. This section discusses three unsupervised classification techniques namely K-means clustering, PCA based K-means clustering and Fuzzy C-Means clustering (FCM).

5.3.1 K-Means Clustering

Mao and Jain et al (1996) defined K-means clustering is used to cluster the pixel intensities in an image into K number of clusters. This offers the segmentation of an image into K segments similar intensities and it provides more automation than manual thresholding of an image.

Assume the size of an image is $m \times n$, convert to a vector with $(m \times n)$ rows and 1 column. With the images, a 3-dimensional feature vector per pixel is used. K-means puts pixels into K number of clusters based on similarities of intensity values. Finally got a set of different segmented image, where each segment is relatively homogeneous in terms of pixel intensities. K-means clustering is used for a simple technique for image classification.

The following are the main three steps of K-Means clustering until convergence.

Repeat the following steps until convergence.

- Determine the centroid coordinate.
- Determine the distance of each object to the centroids.
- Cluster the object based on minimum distance.

Finally, to minimize the following objective function the squared error function is used.

$$A = \sum_{i=1}^m \sum_{j=1}^n \|x_j^i - c_i\|^2 \quad (5.1)$$

where $\|x_j^i - c_i\|^2$ is a distance measure between a data point x_j^i and the cluster center c_i .

The design for implementing K-means clustering technique is shown in Figure 5.3.

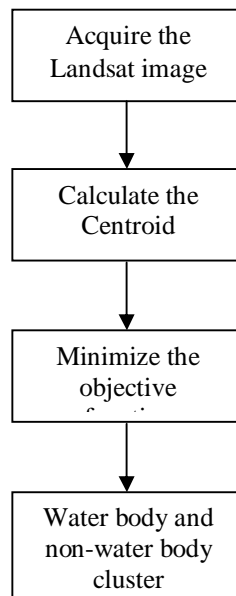


Figure 5.3 K-means clustering – system design

5.3.2 PCA based K-Means Clustering

Thanh et al (2005) defined PCA based K-means clustering is a statistical technique widely used for dimension reduction. Usually the clustering methods are developed for different purposes. Clustering algorithms used for unsupervised classification of remote sensing data vary according to the efficiency with which clustering takes place. The unsupervised clustering provides the cluster information about the water body and non-water body in a relatively quick manner.

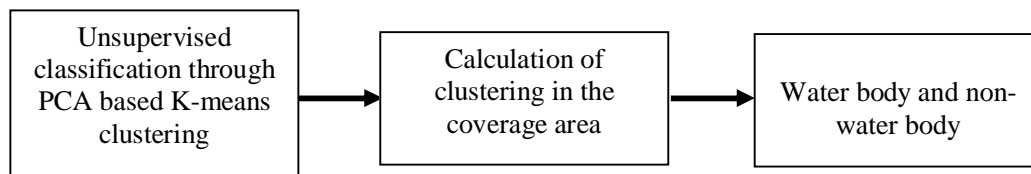


Figure 5.4 Clustering modules

The most important aspect of image classification is finding groups in data. Pixels with similar intensities forms clusters in images. Gray values are specifically used for this purpose. The K-means algorithm has some further refinements for its applications like change detection, land cover mapping, etc., by splitting and merging of clusters. This is illustrated in Figure 5.4.

First, the given image values are preprocessed by using PCA. Using the most important components of PCA, the image information is mapped into the new feature space. Then, the K-means algorithm is applied to the data in the feature space. The final objective is to distinguish the different clusters using eigen values. Clusters are grouped if its standard deviation exceeds a threshold and the number of pixels is twice for the minimum number of pixels. The main intention of K-means algorithm is to reduce the cluster variability. The objective function is to find the sum of square distance between cluster centre and its assigned pixel value as defined in Equation (5.2).

$$F = \sum_{i=0}^n [x_i - C(x_i)]^2 \quad (5.2)$$

where, x_i is the pixel value assigned to mean value of the cluster $C(x_i)$. Next to determine the error as defined in Equation (5.3). Minimizing the error is equivalent to minimizing the sum of squared distances.

$$\text{Error} = \frac{\sum_{i=0}^n [x_i - C(x_i)]^2}{(N - C)} \quad (5.3)$$

where, N indicates number of pixels, C specifies the expected number of clusters. K-means is very responsive to initial values. It is often not obvious that the clustering with the lesser Mean Squared Error (MSE) is truthfully the better classification. Thus, the results obtained have aided in attaining this objective and thereby PCA based K-means clustering has been efficiently applied for the classification analysis.

5.3.3 Fuzzy C-Means Clustering

Rui and Donald (2005) discussed Fuzzy C-Means (FCM) clustering algorithm permits a data to belong to more than two clusters. This method is frequently used in change detection, pattern recognition and classification. It is mainly aimed to minimize the objective function as defined in the Equation (5.4).

$$A_m = \sum_{i=1}^N \sum_{j=1}^C a_{ij}^m \|x_j - c_i\|^2, \quad 1 \leq m < \infty \quad (5.4)$$

where $m \geq 1$, a_{ij} is the degree of membership of x in the cluster j , x_j is the j^{th} dimensional measured data, c_i is the cluster center, and $\|x_j - c_i\|$ expressing the similarity between measured data and the cluster center.

The objective function of the optimization yields the fuzzy partitioning shown above, with the updation of membership function a_{ij} , defined in Equation (5.5) and the cluster centers, c_j .

$$a_{ij} = \frac{1}{\sum_{m=1}^c \left[\frac{\|x_j - c_i\|}{\|x_j - c_m\|} \right]^{\frac{2}{m-1}}} \quad (5.5)$$

The iteration will stop until $\max_{ij} \{ |a_{ij}^{k+1} - a_{ij}^k| \} < \epsilon$, $0 < \epsilon < 1$, k is the number of steps to repeat the iteration. The following Figure 5.5 depicts the system design for implementing Fuzzy C-Means clustering.

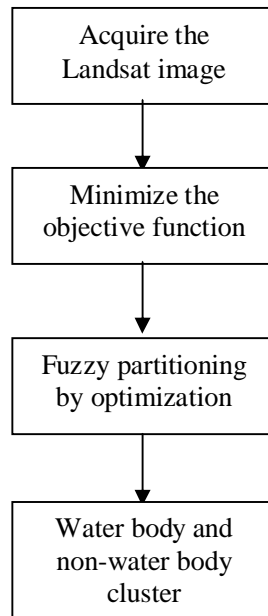


Figure 5.5 Fuzzy C-Means Clustering – system design

5.3.3.1 Fuzzy C-means implementation steps

- The FCM function is called upon which takes the pixel array and the number of clusters as input.

- The FCM function returns the objective function values, membership grades and the cluster centers as output.
- Based on the degree of membership the data points are moved into different clusters.
- Given a data set, there are n training samples. The values for the parameter $X = x_1, x_2, \dots, x_n$ denoted as $Y = \text{sort}[X] = y_1, y_2, \dots, y_n$. The parameter Y indicates the ascending order of the parameter X . Once the X values are sorted it is easy to find out the association between adjacent values.
- Next determine the difference between the set of training data as mentioned in Equation (5.6).

$$d_i = Y_{i+1} - Y_i, \quad i = 1, 2, \dots, n-1. \quad (5.6)$$

where Y_i and Y_{i+1} are adjacent values.

- Calculate the adjacent value similarities by using Equation (5.7).

$$S_i = \begin{cases} 1 - \frac{d_i}{CP \times \sigma_s}, & d_i \leq CP \times \sigma_s \\ 0, & \text{otherwise} \end{cases} \quad (5.7)$$

where d_i is the difference, σ_s is the standard deviation of d_i and

CP is the control parameter.

- A threshold value σ_s divides adjacent values into classes. Determination of clusters can be recapitulated by a rule. This can be expressed in Equation (5.8) as,

$$\begin{aligned}
&\text{IF}(s_i > \sigma) \text{ THEN } Y_i, Y_{i+1} \in CP_i \\
&\quad \text{ELSE } Y_i \in CP_i, Y_{i+1} \in CP_{i+1}
\end{aligned} \tag{5.8}$$

where CP_i and CP_{i+1} denote two dissimilar classes for the input or output parameter.

5.4 THE SUPERVISED CLASSIFICATION

Huang et al (2009) presented supervised classification identifies the specific area of interest i.e., water body and non-water body in the image. The supervised classification is much more accurate for mapping classes, but depends heavily on the cognition and skills of the image specialist. The strategy is simple: the specialist must recognize conventional classes or meaningful classes in a scene from prior knowledge, such as personal experience with what's present in the scene, or more generally, the region it's located in, by experience with thematic maps, or by on-site visits. This familiarity allows the individual making the classification to choose and set up discrete classes and then, assign them category names.

As a rule, the classifying person also locates specific training sites on the image to identify the classes. The resulting training sites are areas representing each known land cover category that appear fairly homogeneous on the image. For each class thus outlined, mean values and variances of the each band used to classify them are calculated from all the pixels enclosed in each site. More than one polygon is usually drawn for any class. The classification program then acts to classify the data representing each class. When the classification for a class is plotted as a function of the band the result is a spectral signature or spectral response curve for that class. The multiple spectral signatures so obtained are for all of the materials within the site that interact with the incoming radiation.

Classification now proceeds by statistical processing in which every pixel is compared with the various signatures and assigned to the class whose signature comes closest. Many of the classes for the satellite images are almost self-evident in portraying ocean water, waves, beach, marsh, shadows. For example, difference between ocean and bay waters, but their gross similarities in spectral properties would probably make separation difficult. Some classes are broad-based, representing two or more related surface materials that might be separable at high resolution but are inexactly expressed in the image. Thus, the supervised classification has an edge over the unsupervised methodology. Learning Vector Quantization (LVQ) and the Support Vector Machines (SVM) are the two supervised classification methodologies implemented to perform the analysis for the water body and non-water body classification.

5.4.1 Learning Vector Quantization

Zhou Kaili (2005) Learning Vector Quantization (LVQ) is also used in feature vector dimension reduction. Here is the chance to optimize training data through reducing the number of samples for this analysis. LVQ is a variation of the well-known Self Organizing Map (SOM) architecture. The SOM system is known as a Kohonen network. This has a feed-forward structure with a single computational layer of neurons arranged in rows and columns. Each neuron is fully connected to all the source units in the input layer. The architecture is being depicted in the Figure 5.6. A one dimensional map will just have a single row or column in the computational layer. The feature map is being derived from the spatially continuous input space, in which input the vectors live, to the low dimensional spatially discrete output space, which is formed by arranging the computational neurons into a grid.

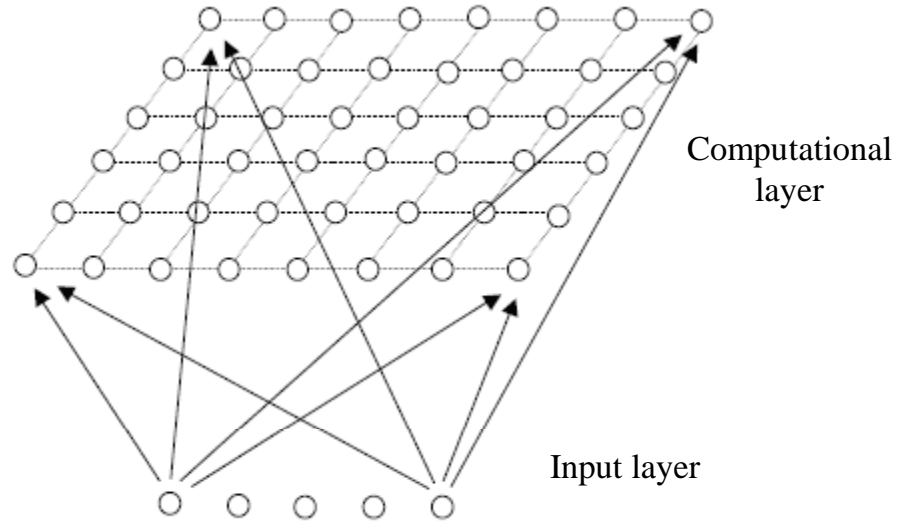


Figure 5.6 Arrangement of neurons in multi-dimensional SOM architecture

5.4.1.1 Stages of LVQ

The different stages of LVQ are

- Step 1:** Initialization – Assign the initial weight vector w_j by selecting the random values.
- Step 2:** Sampling – Describe a sample input vector x from the input space. Here the network chooses five texture features as input to classify the two classes.
- Step 3:** Matching – Find weight vector closest to the input vector named as winning neuron $I(x)$, which is defined as in Equation (5.9).

$$\sum_{i=1}^n (x_i - w_{ji})^2 \quad (5.9)$$

Step 4: Updating – Apply the following weight update function to update the weights as shown in Equation (5.10).

$$\Delta w_{ji} = \eta T_{j,I(x)}(x_i - w_{ji}) \quad (5.10)$$

where $T_{j,I(x)}$ is a Gaussian neighbourhood and η is the learning rate.

Step 5: Continuation – Repeat the steps 2 to 5 to reach the best accuracy of input space.

5.4.1.2 Properties of the feature map

Once the SOM algorithm has converged, the feature map displays important statistical characteristics of the input space. Given an input vector x , the feature map ϕ provides a winning neuron $I(x)$ in the output space and the weight vector $W_{I(x)}$ provides the coordinates of the image of that neuron in the input space as shown in Figure 5.7.

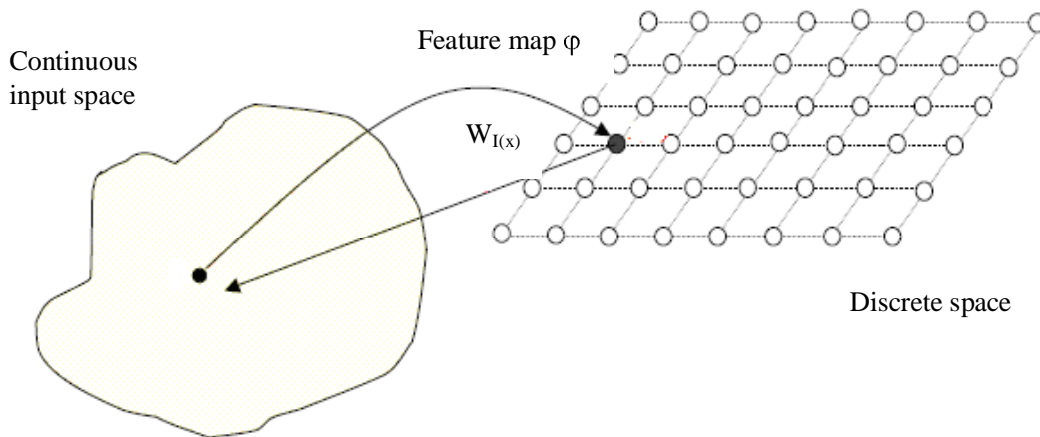


Figure 5.7 Topological ordering and density matching of the feature map

5.4.1.3 Basics of vector quantization

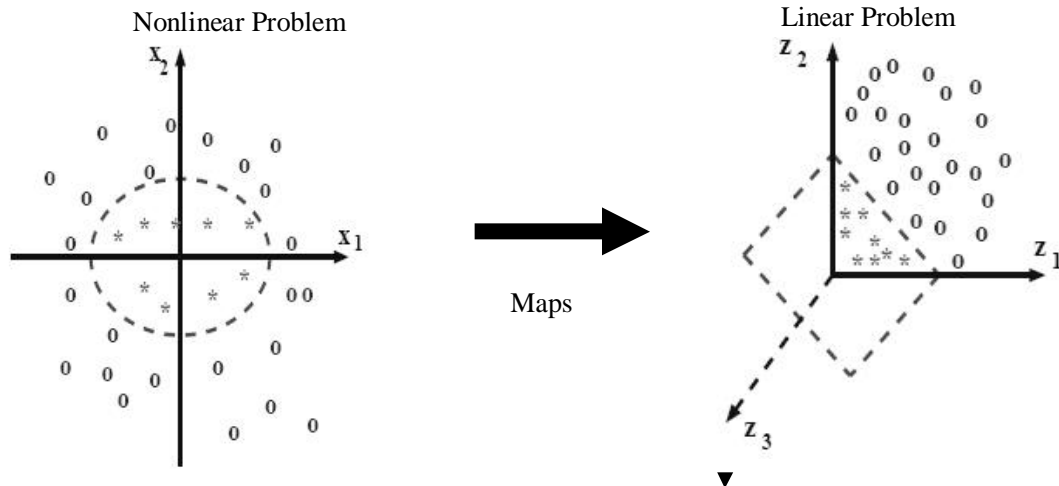
The main aim of using a self organizing map is to encode a large set of input vectors $\{x\}$ by finding a smaller set of “representatives” or “prototypes” or “code-book vectors” $\{w_{I(x)}\}$ that provide a good approximation to the original input space. This is the basic idea of vector quantization theory. The motivation of which is dimensionality reduction or data compression. In effect, the error of the vector quantization approximation is the total squared distance between the input vectors $\{x\}$ and their representatives $\{w_{I(x)}\}$ as defined in Equation (5.11).

$$D = \sum_x \|x - w_{I(x)}\|^2 \quad (5.11)$$

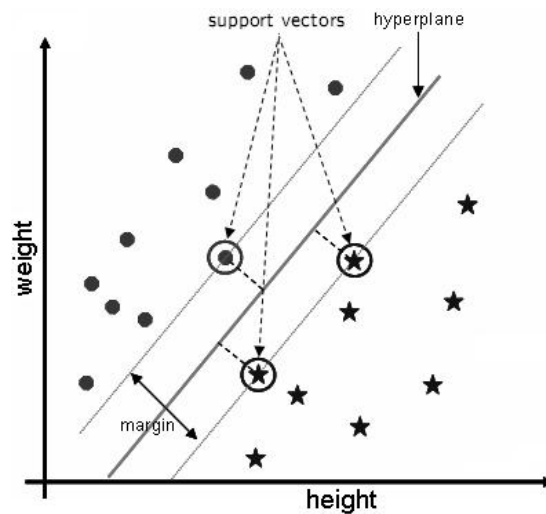
A gradient descent style minimization of D does lead to the SOM weight update algorithm, which confirms that it is generating the best possible discrete low dimensional approximation to the input space.

5.4.2 Support Vector Machine classifier

Support Vector Machines were introduced by Vladimir Vapnik (1995). A support vector machine (SVM) is a concept for a set of related supervised learning methods that analyze data, recognize patterns and then used for classification and regression analysis. The classification problem can be restricted to consideration of the two-class problem without loss of generality. The goal is to separate the two classes by a function which is induced from available training data sets.



SVM Hyperplane

**Figure 5.8 Working of SVM**

For each given input, the SVM determines if the input is a member of water body or non-water body class. This makes SVM as a linear classifier. The goal is to separate the two classes without loss of generality by a function which is induced from available training data sets. The task is to produce a classifier that will work in a generalized manner. The application of SVM for the desired problem is minimizing the error through maximizing the margin which means that it maximizes the distance between it and the nearest data point of each class. Since SVMs are known to generalize well even in high

dimensional spaces under small training samples, this linear classifier is termed as the optimal separating hyper plane as shown in Figure 5.8.

The SVM takes a set of input data and then predicts, for each given input, which of two possible classes. Given a set of training data, each marked as belonging to one of two categories, an SVM training algorithm builds a model that assigns new data into one category or the other.

SVM is used to construct a decision plane called the hyper plane which separates the water body class from non-water body class. Figure 5.9 illustrates the SVM classifier for two classes: water body and non-water body.

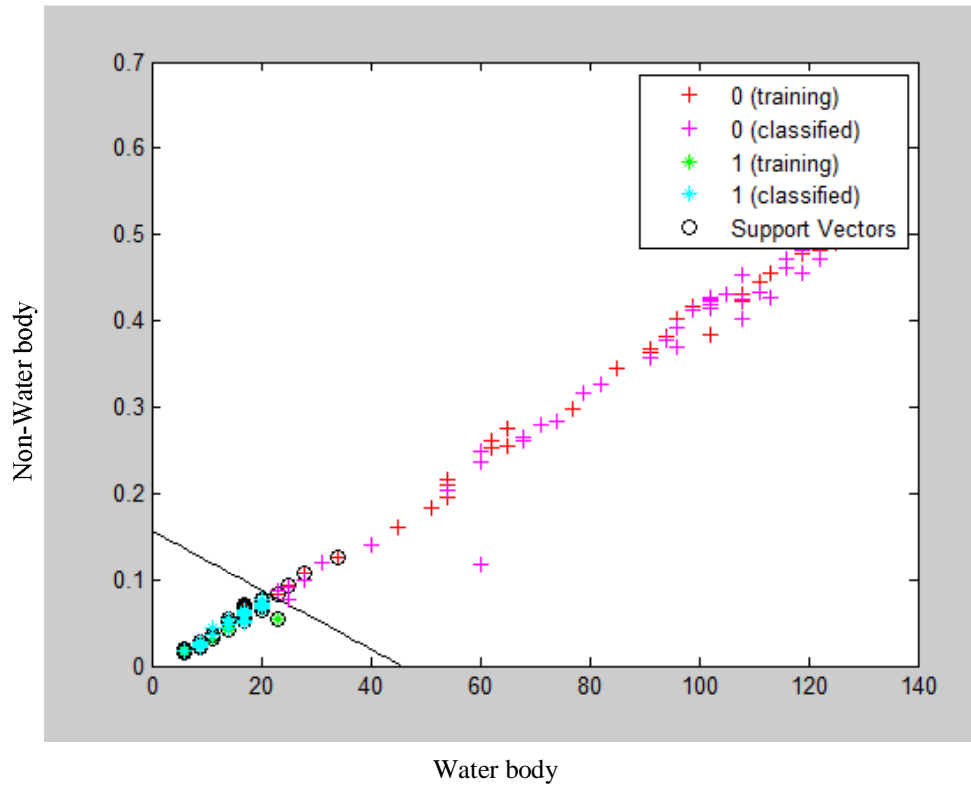


Figure 5.9 SVM Classifier

5.4.2.1 SVM -Background

Given l training examples $\{x_i, y_i\}$, $i = 1, \dots, l$, where each example has d inputs ($x_i \in \mathbb{R}^d$), and a class label with one of two

values ($y_i \in \{-1, 1\}$). Now, all hyperplanes in R^d are parameterized by a vector (w), and a constant (b), expressed in the equation (5.12) as follows

$$w \cdot x + b = 0 \quad (5.12)$$

Given such a hyperplane (w, b) that separates the data, this gives the function defined in equation (5.13) as

$$f(x) = \text{sign}(w \cdot x + b) \quad (5.13)$$

which correctly classifies the training data (and hopefully other “testing” data it hasn’t seen yet). However, a given hyperplane is represented by (w, b) is equally expressed by all pairs $\{\lambda w, \lambda b\}$ for $\lambda \in R_+$. So define the canonical hyperplane to be that which separates the data from the hyperplane by a “distance” of at least 1. That is, consider those that satisfy equation (5.14) and (5.15):

$$x_i \cdot w + b \geq +1 \text{ when } y_i = +1 \quad (5.14)$$

$$x_i \cdot w + b \leq -1 \text{ when } y_i = -1 \quad (5.15)$$

or more compactly:

$$y_i (x_i \cdot w + b) \geq 1 \quad \forall i \quad (5.16)$$

All such hyperplanes have a functional distance ≥ 1 (quite literally, the function’s value is ≥ 1). This shouldn’t be confused with the geometric or Euclidean distance (also known as the margin). For a given hyperplane (w, b), all pairs $\{\lambda w, \lambda b\}$ define the exact same hyperplane, but each has a different functional distance to a given data point. To obtain the geometric distance from the hyperplane to a data point, it can be normalized by the

magnitude of w .

Intuitively, the hyperplane that maximizes the geometric distance to the closest data points.

5.5 ACCURACY CALCULATION

Defries and Chan (2000) described the accuracy of SVM classification can be calculated in terms of classified rate, correct rate and error rate. The classified rate is the ratio of classified samples to the total number of samples. The correct rate is the ratio of correctly classified samples to the classified samples and the error rate is the ratio of incorrectly classified samples to the classified samples. These are defined as in Equations (5.17) – (5.19) as follows:

$$\text{ClassifiedRate} = \frac{\text{Classified Samples}}{\text{Total no of samples}} \quad (5.17)$$

$$\text{Correct Rate} = \frac{\text{Correctly Classified Samples}}{\text{Classified Samples}} \quad (5.18)$$

$$\text{Error Rate} = \frac{\text{Incorrectly Classified Samples}}{\text{Classified Samples}} \quad (5.19)$$

Powell et al (2004) and Congalton et al (2002) have discussed the accuracy of the classification can also be calculated in terms of Receiver Operating Characteristics (ROC) terminology, true positive (TP), false positive (FP), true negative (TN) and false negative (FN). True positive rate is the proportion of positive cases that were correctly identified and false positive rate is the proportion of negatives cases that were incorrectly

classified as positive. Classification accuracy is the proportion of the total number of predictions that were correct.

Sensitivity is the true positive, the region of water body which is correctly classified as positive. The true negative is specificity, the region of water body who actually are without correctly classified as negative. The implication of this is false positive and false negative can also be measured. This is an important assumption of ROC analysis, making ROC useful for highly prevalent classification. The typical ROC curve places FP on the horizontal axis and TP on the vertical axis.

5.6 EXPERIMENTAL RESULTS AND DISCUSSIONS

5.6.1 Data Sets

This work deals with the Land Remote-Sensing Satellite (LANDSAT) images taken from different time frames of Kochi, Kanyakumari, Kolkata Visakhapatnam and Sydney regions.

5.6.2 Texture Features to be Subjected

The Figure 5.10 shows the texture features such as energy, entropy, contrast, inverse difference moment and directional moment extracted using GLCM along with the corresponding classes such as water body and non-water body.

	A	B	C	D	E	F
1	energy	entropy	contrast	idm	dm	class
2	0.3553	6.4325	0.1991	5.99E+04	282.5805	1
3	0.355	6.3428	0.1337	6.14E+04	239.758	1
4	0.434	5.0181	0.1403	6.28E+04	298.3901	1
5	0.5126	5.8282	0.2411	6.02E+04	375.6327	1
6	0.3639	5.9732	0.2718	5.93E+04	377.373	1
7	0.3029	6.8499	0.0858	6.83E+04	177.7433	1
8	0.3644	6.5045	0.082	6.27E+04	184.4153	1
9	0.2372	6.5979	0.0711	6.31E+04	146.9419	1
10	0.3571	6.6991	0.0576	6.36E+04	141.1339	1
11	0.2527	6.5253	0.1882	5.99E+04	293.3726	1
12	0.1487	7.1408	0.416	5.40E+04	441.3777	2
13	0.1966	6.9241	0.2857	5.66E+04	331.4446	2
14	0.2345	6.8485	0.1857	5.95E+04	267.7715	2
15	0.1592	7.0073	0.4021	53987	408.3942	2
16	0.1684	6.8769	0.4213	53156	403.316	2
17	0.2426	6.7398	0.2239	5.82E+04	268.7716	2
18	0.1974	7.062	0.2206	5.88E+04	318.4569	2
19	0.1947	6.8828	0.2881	5.45E+04	321.4467	2
20	0.1246	7.0946	0.5568	5.09E+04	502.0053	2
21	0.2044	6.9699	0.229	5.89E+04	320.0672	2

Figure 5.10 Input data consisting of five texture features with the corresponding classes

5.6.3 Training using Neural Network

Then the input samples are trained using neural network. The numbers of input training data sets are 1026. The network is designed by 5 input layers, 30 hidden layers and 1 output layer. The activation function of each output neuron is a radial function, i.e., a monotonously decreasing function.

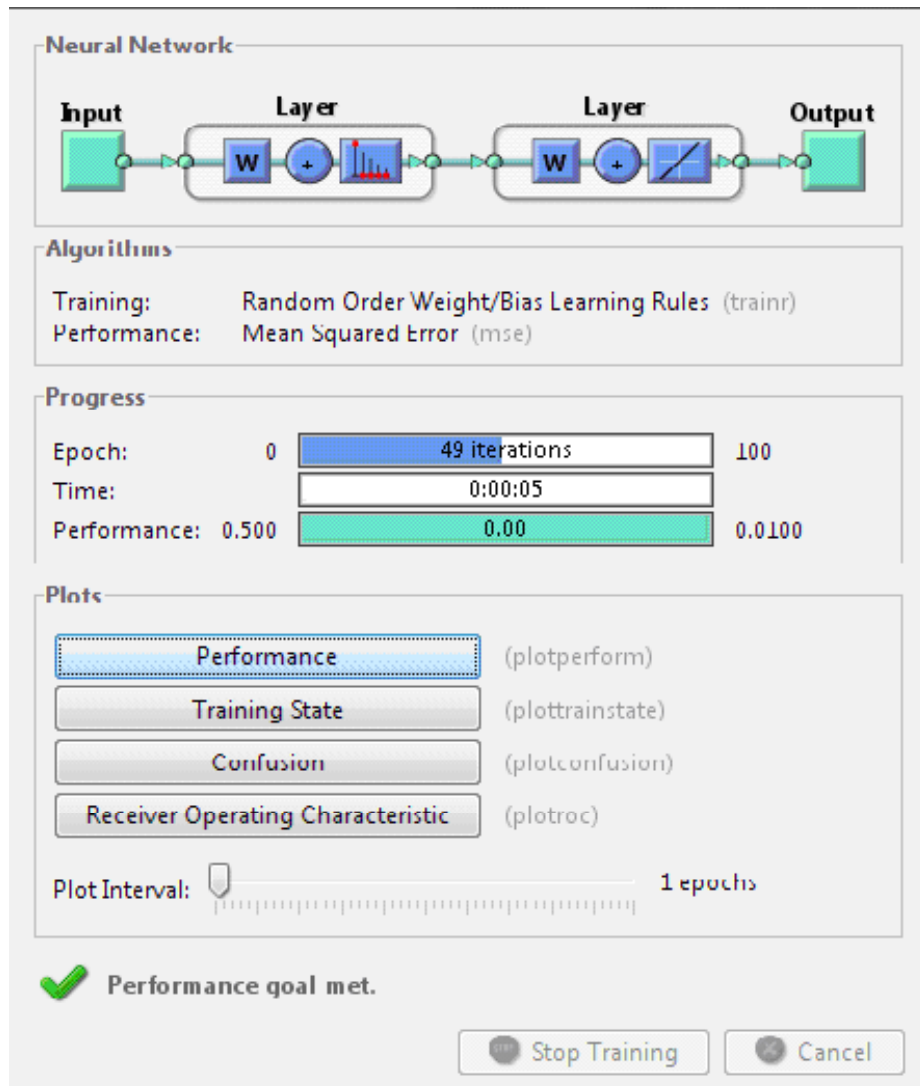
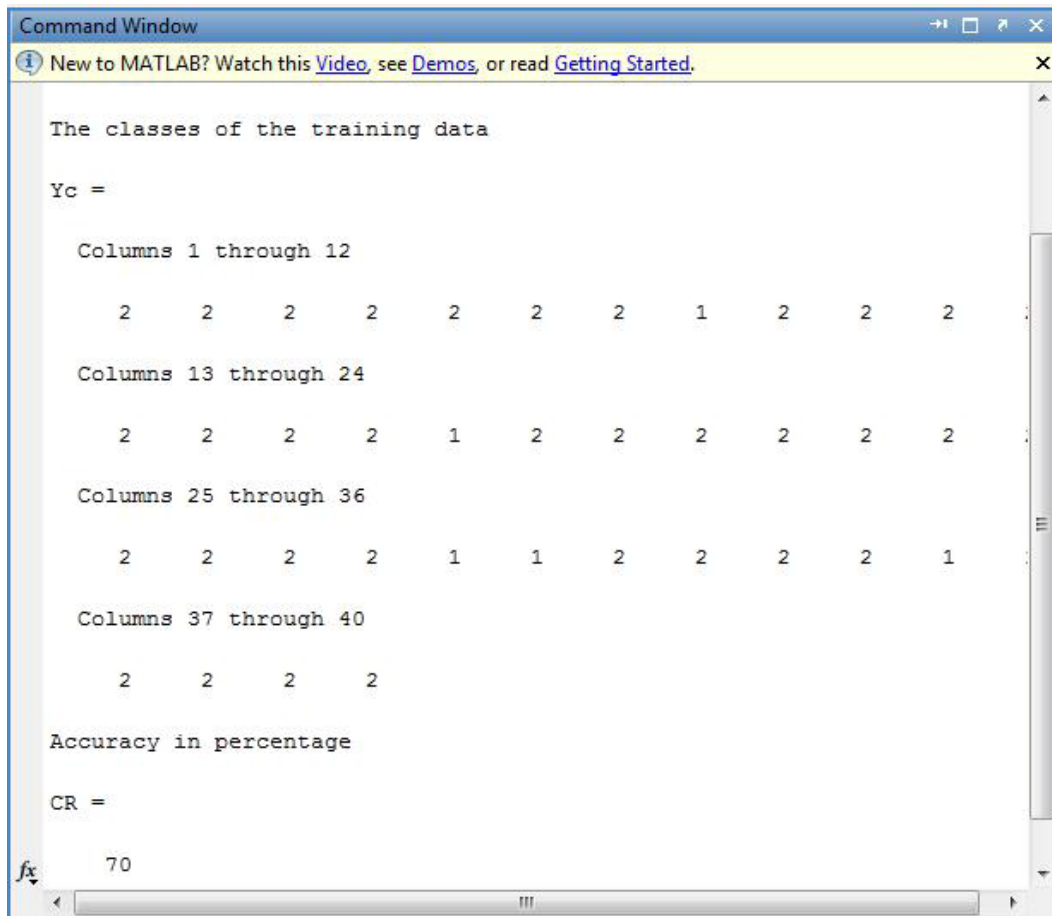


Figure 5.11 Training using neural network

The term 'Performance goal met' indicates that the training data satisfies the necessary and sufficient conditions in order to achieve the maximum accuracy. Thus, there has been a successful result meeting 100% accuracy which is shown in Figure 5.11 and Figure 5.12.



```

Command Window
New to MATLAB? Watch this Video, see Demos, or read Getting Started.

The classes of the training data

Yc =

Columns 1 through 12
     2     2     2     2     2     2     2     1     2     2     2
Columns 13 through 24
     2     2     2     2     1     2     2     2     2     2     2
Columns 25 through 36
     2     2     2     2     1     1     2     2     2     2     1
Columns 37 through 40
     2     2     2     2

Accuracy in percentage

CR =

    70
  
```

Figure 5.12 MSE and accuracy in percent of the classified results

5.6.4 Results of Classification

The support vector machine classifies the images into water body and non-water body and this shows that the resolution enhanced image gives better accuracy than the denoised image. Figure 5.13 to Figure 5.17 show the water body and non-water classified result of Kochi, Kanyakumari, Kolkata, Visakhapatnam and Sydney region. In the output image, white colour shows the water body and black colour shows the non-water body region.



(a) Resolution enhanced input image



(b) Classified output

Figure 5.13 Experimental results of (a) resolution enhanced input image and (b) Water body and non-water body classified result of Kochi region



(a) Resolution enhanced input image



(b) Classified output

Figure 5.14 Experimental results of (a) resolution enhanced input image and (b) water body and non-water body classified result of Kanyakumari region

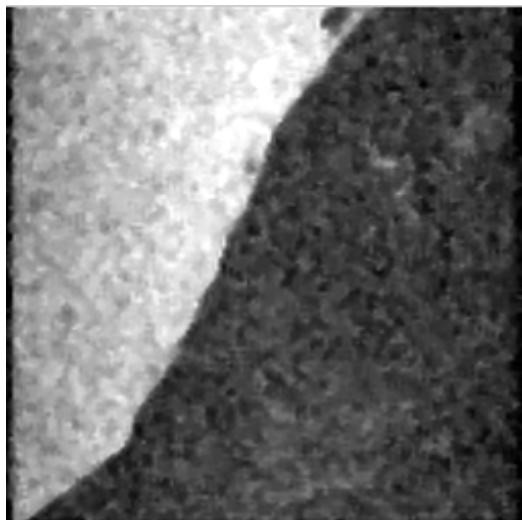


(a) Resolution enhanced input image

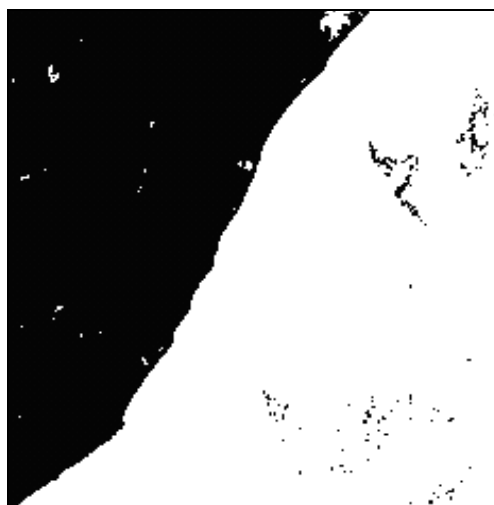


(b) Classified output

Figure 5.15 Experimental results of (a) resolution enhanced input image and (b) water body and non-water body classified result of Kolkata region

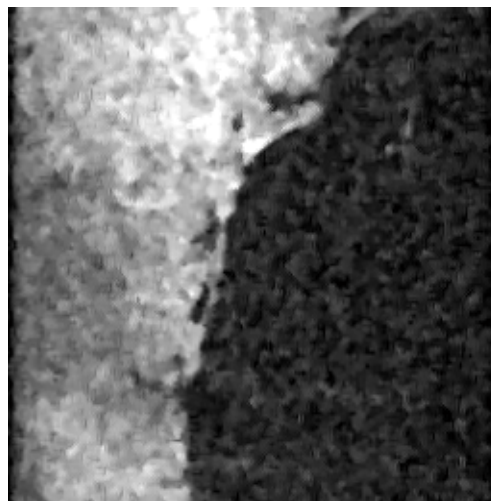


(a) Resolution enhanced input image



(b) Classified output

Figure 5.16 Experimental results of (a) resolution enhanced input image and (b) water body and non-water body classified result of Visakhapatnam region



(a) Resolution enhanced input image



(b) Classified output

Figure 5.17 Experimental results of (a) resolution enhanced input image and (b) water body and non-water body classified result of Sydney region

5.6.5 Accuracy Calculation

The support vector machine classifies the images into water body and non-water body and this shows that the resolution enhanced image gives better accuracy than the denoised image. The classification accuracy of denoised images and resolution enhanced images are shown in Table 5.1.

Table 5.1 Classification accuracy of denoised and DWT based interpolation technique resolution enhanced images

Sl. No	Region Name	HDL Denoised Image			Resolution Enhanced Image		
		Classified Rate	Correct Rate	Error Rate	Classified Rate	Correct Rate	Error Rate
1	Kochi	100	45	55	100	65	35
2	Kanyakumari	100	60	40	100	85	15
3	Kolkata	100	40	60	100	55	45
4	Vishakhapatnam	100	55	45	100	60	40
5	Sydney	100	60	40	100	65	35

5.6.5.1 ROC Analysis

The Receiver Operating Characteristics (ROC) analysis is a technique for visualizing, organizing and selecting classifiers based on their performance. ROC curve shows true positive (TP) rate versus false positive (FP) rate (sensitivity versus specificity) for different thresholds of the classifier output. This analysis can be used to find the threshold value that

maximizes the classification accuracy or to assess how the classifier performs in the regions of high sensitivity and high specificity.

The ROC curve can compute values for various criteria to plot either on the X-axis or on the Y-axis. This returns values of specificity, or false positive rate in the X-axis and sensitivity, or true positive rate in the Y-axis. All such criteria are described by a confusion matrix.

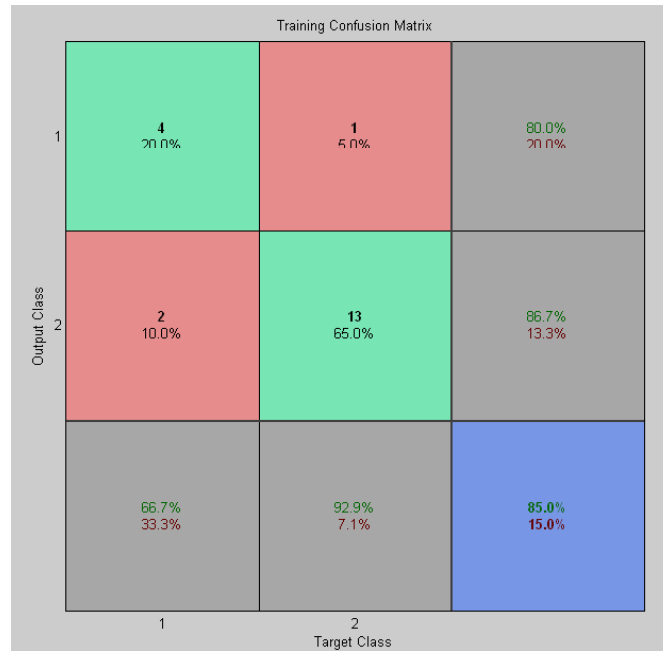
The confusion matrix, C is defined as

$$C = \begin{bmatrix} TP & FN \\ FP & TN \end{bmatrix} \quad (5.15)$$

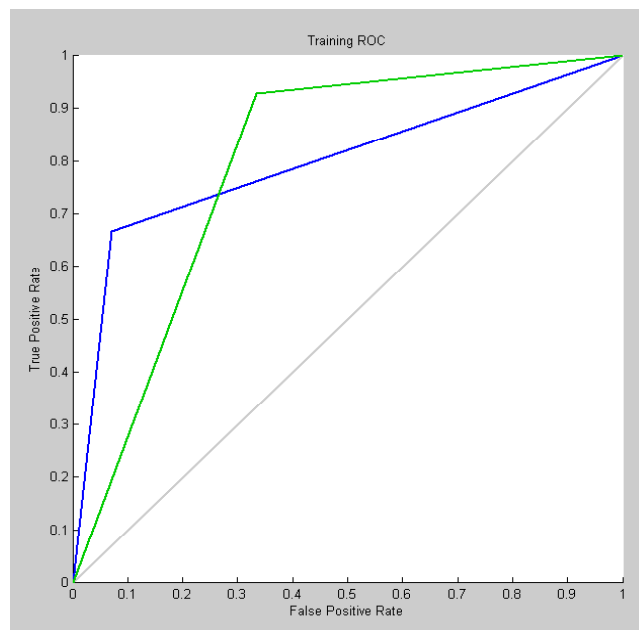
where TP - True Positive, FP - False Positive, FN - False Negative and TN - True Negative.

The first row of the confusion matrix defines how the classifier identifies instances of the positive class: $C(1,1)$ is the count of correctly identified positive instances and $C(1,2)$ is the count of positive instances misidentified as negative.

The performance of the SVM classifier is also evaluated using ROC curve. The ROC curve and confusion matrix of various regions are depicted in Figures 5.18 to 5.22.

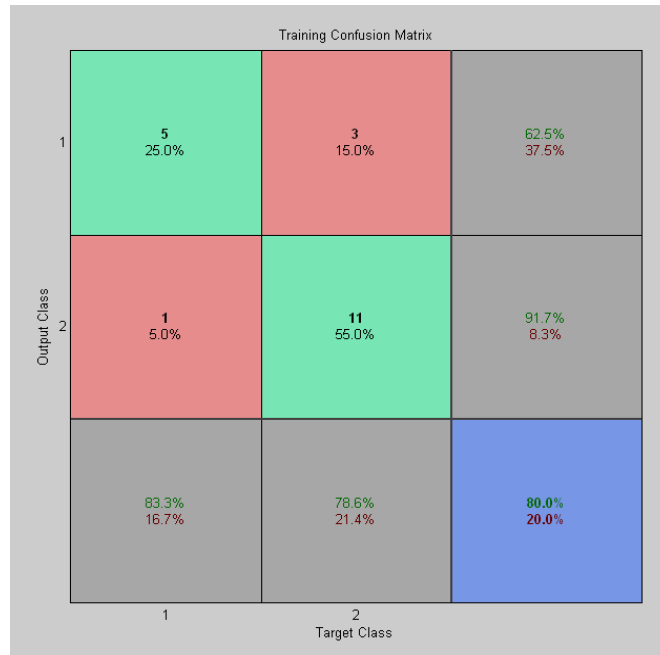


(a) Confusion matrix

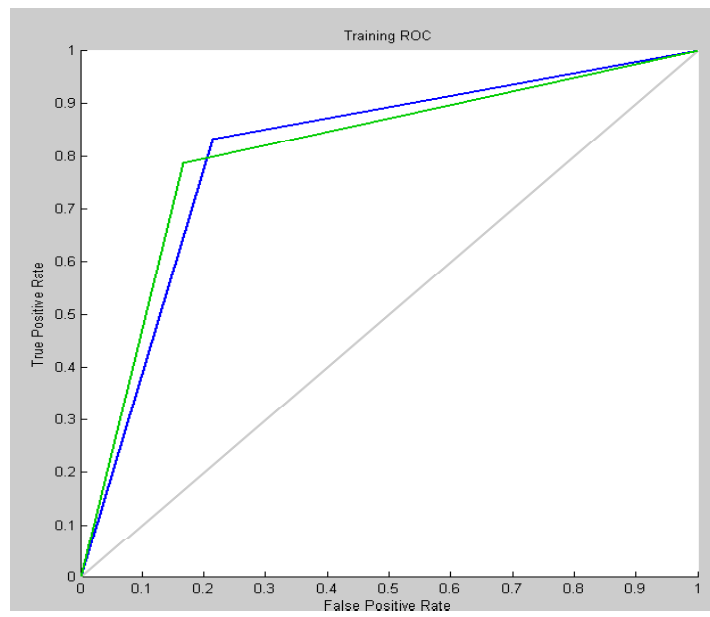


(b) ROC curve

Figure 5.18 Performance analysis (a) confusion matrix and (b) ROC curve of Kochi region

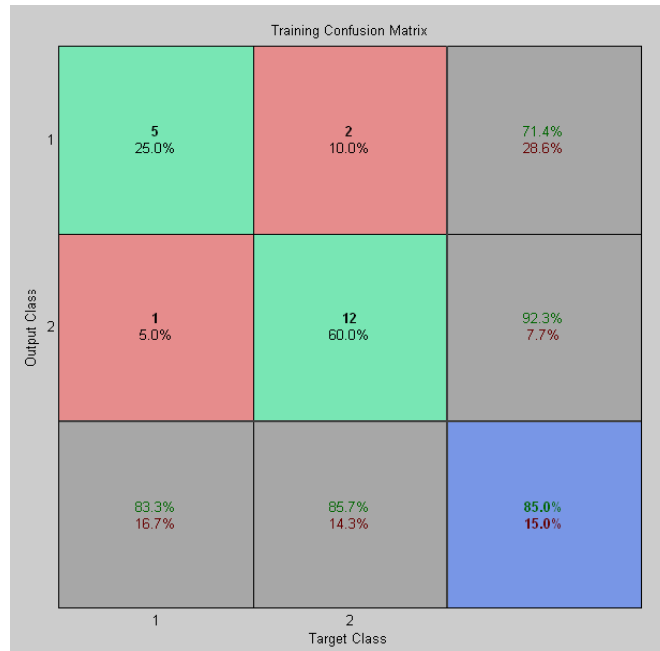


(a) Confusion matrix

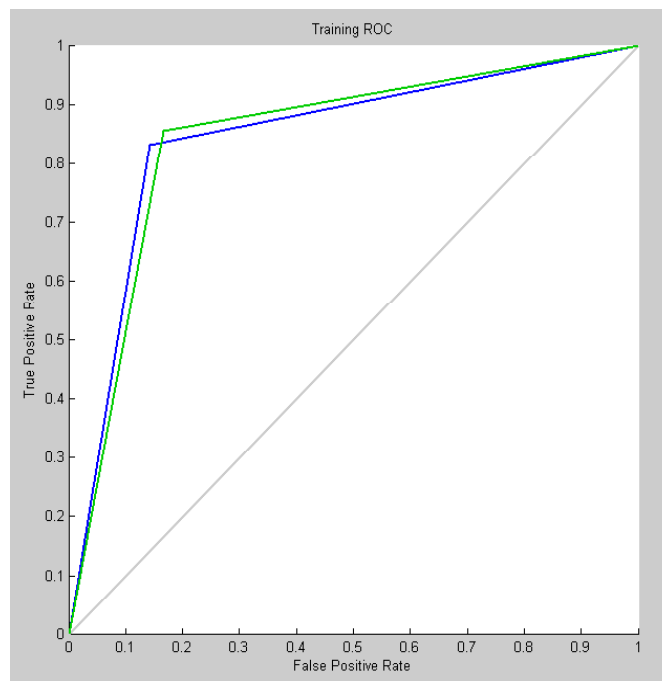


(b) ROC curve

Figure 5.19 Performance analysis (a) confusion matrix and (b) ROC curve of Kanyakumari Region

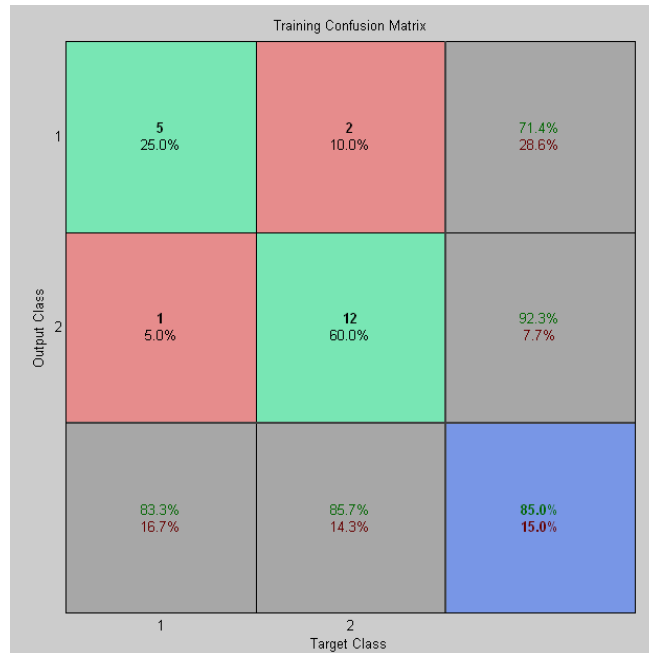


(a) Confusion Matrix

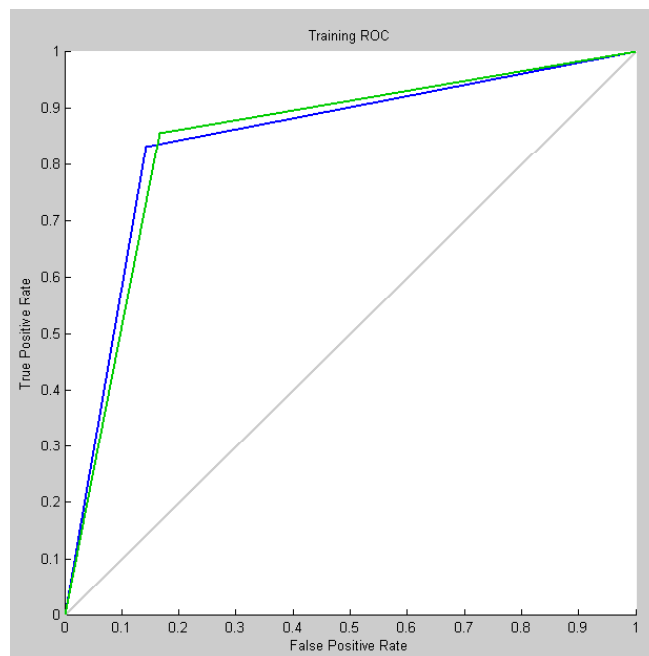


(b) ROC curve

Figure 5.20 Performance analysis (a) confusion matrix and (b) ROC curve of Kolkata Region

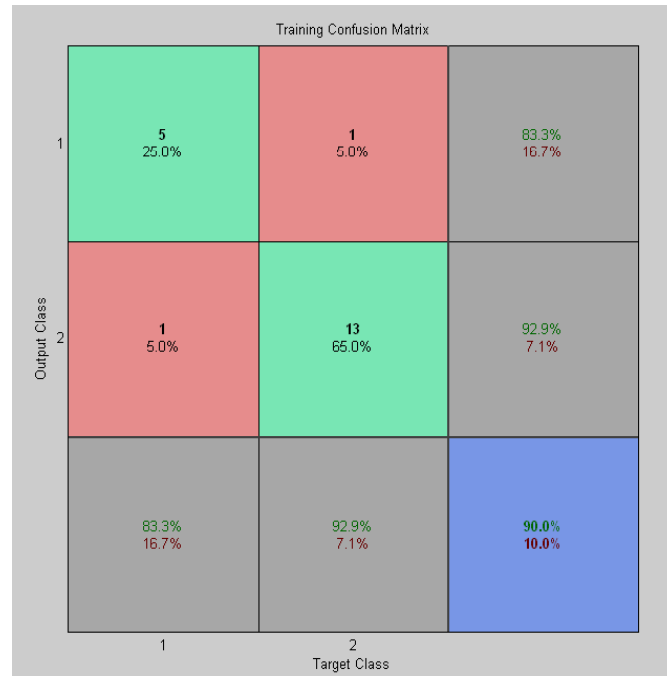


(a) Confusion Matrix

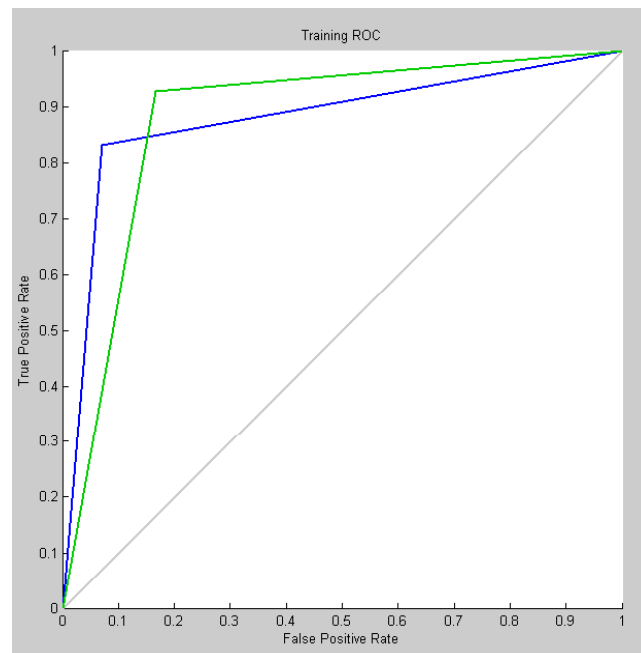


(b) ROC curve

Figure 5.21 Performance analysis (a) confusion matrix and (b) ROC curve of Vishakhapatnam region



(a) Confusion matrix



(b) ROC curve

Figure 5.22 Performance analysis (a) confusion matrix and (b) ROC curve of Sydney region

The ROC analysis results show that the Kochi region has a sensitivity of 80% and specificity of 86.7% and the accuracy is 85%, Kanyakumari region has a sensitivity of 62.5% and specificity of 91.7% and the accuracy is 80%, Kolkata and Vishakhapatnam region have a sensitivity of 71.4% and specificity of 92.3% and the accuracy is 85% and Sydney region has a sensitivity of 83.3% and specificity of 92.9% and the accuracy is 90%.

5.6.6 CPU Time Calculation

The complexity of the proposed techniques, Hybrid Directional Lifting and DWT based Interpolation techniques are analyzed based on the CPU time or process time. The CPU time of a function is the amount of time (in seconds) for which a central processing unit is used to process the instructions of a computer program. Figure 5.23 shows the computation time of HDL and DWT based resolution enhancement techniques.

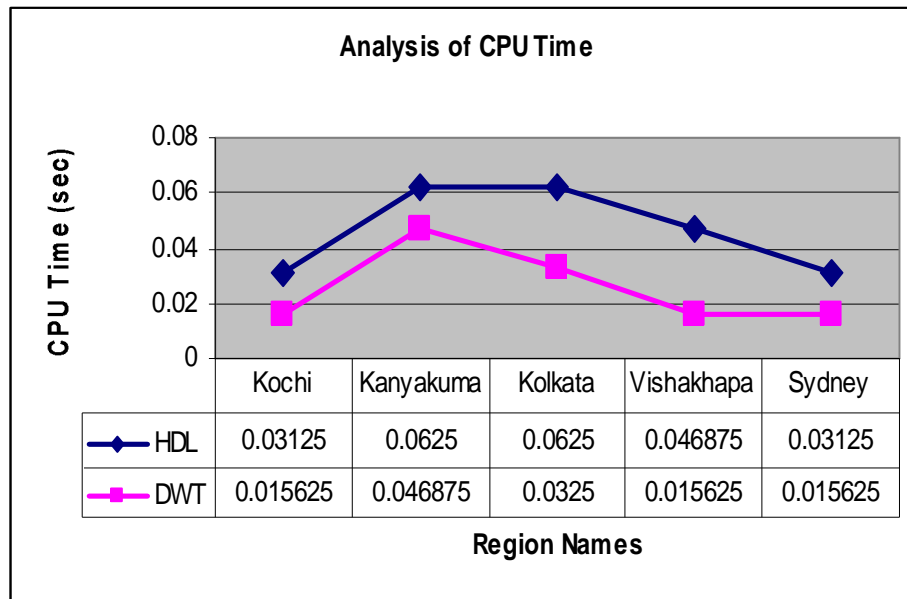


Figure 5.23 Computation time of HDL and DWT based resolution enhancement technique

From the results of computation time, it is inferred that HDL and DWT based interpolation techniques are efficient to execute the algorithm.

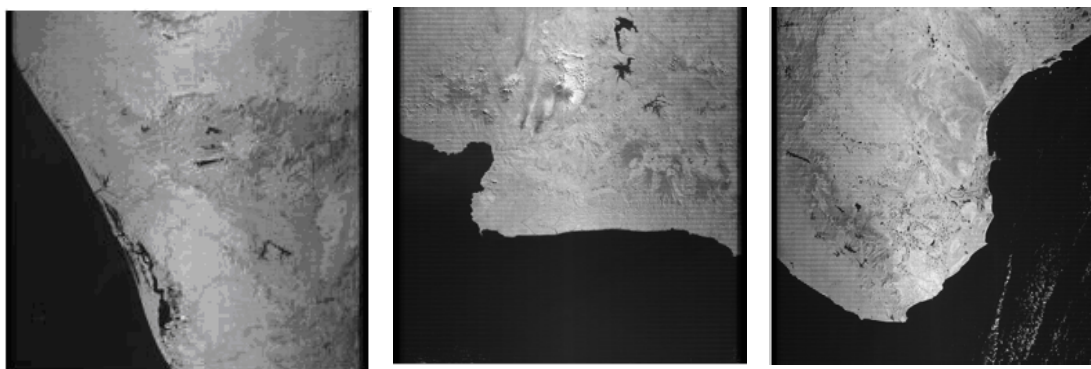
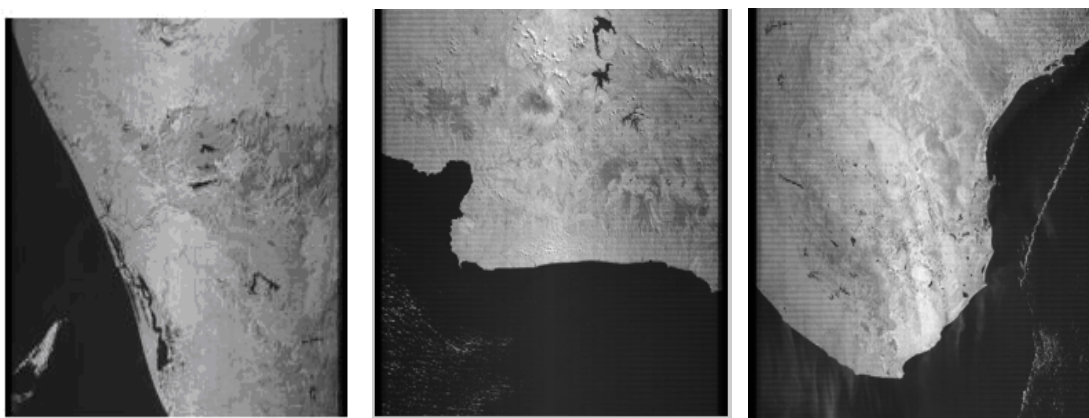
5.7 APPLICATION – CHANGE DETECTION

Change detection is the art of quantifying the changes in synthetic aperture radar images occurring over a period of time. Remote sensing has been instrumental in performing change detection analysis.

Remote sensing and related techniques have a persistent impact on the conduct of real time work. With satellite instruments, it is possible to observe a target repeatedly, thereby contributing effectively to perform change detection in areas of interest. This application mainly focuses on change detection, which happens because of many possible environmental and human actions. SAR images enable direct observation of the land surface at repeated intervals, allowing mapping, monitoring and assessment. Change detection analysis is very effective in long-term planning.

5.7.1 Data Sets

This deals with the Land Remote-Sensing Satellite (LANDSAT) images taken from different time frames of the coastal regions of the world. Some of the sample input study area imageries are shown in Figure 5.24 and Figure 5.25.

**Kochi Region****Indonesia Region****Kanyakumari Region****Figure 5.24 Input landsat images of coastal landscape taken during 2005****Kochi Region****Indonesia Region****Kanyakumari Region****Figure 5.25 Input landsat images of coastal landscape taken during 2010**

5.7.2 Results of Classification through PCA based K-Means Clustering

The input SAR images have been subjected to unsupervised classification performed using a PCA based K-means classifier. Figure 5.26 and Figure 5.27 depict the result of classification which facilitates differentiation of water body from non-water body region. These results have been further utilized in calculating the percentage of coverage area to detect changes over a period of time.

5.7.3 Results of Supervised Classification

The texture features are extracted using GLCM and subjected to LVQ to satisfy the necessary and sufficient conditions to achieve maximum accuracy. The training data has led to results with 100% accuracy.

Subjecting the combination of extracted texture features onto the SVM classifier resulted in 98% accuracy for classifying input data. The classified results are depicted in Figure 5.28.

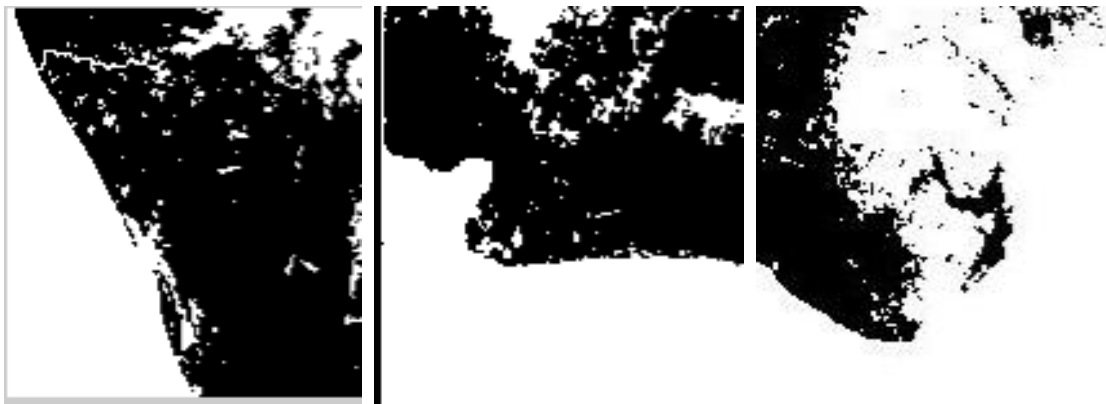


Kochi Region

Indonesia Region

Kanyakumari Region

Figure 5.26 Clustering performed on 2005 images



Kochi Region

Indonesia Region

Kanyakumari Region

Figure 5.27 Clustering performed on 2010 images

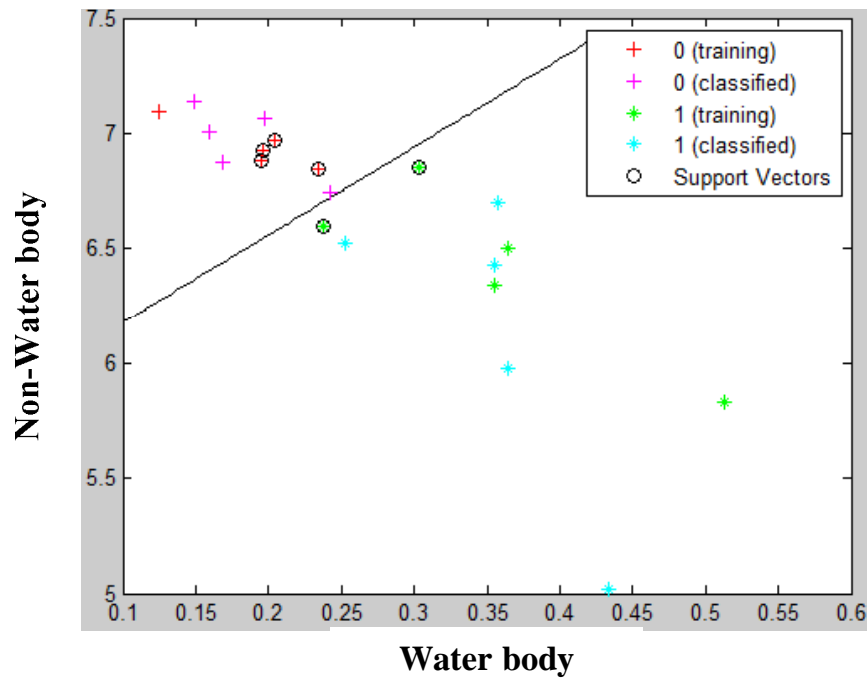
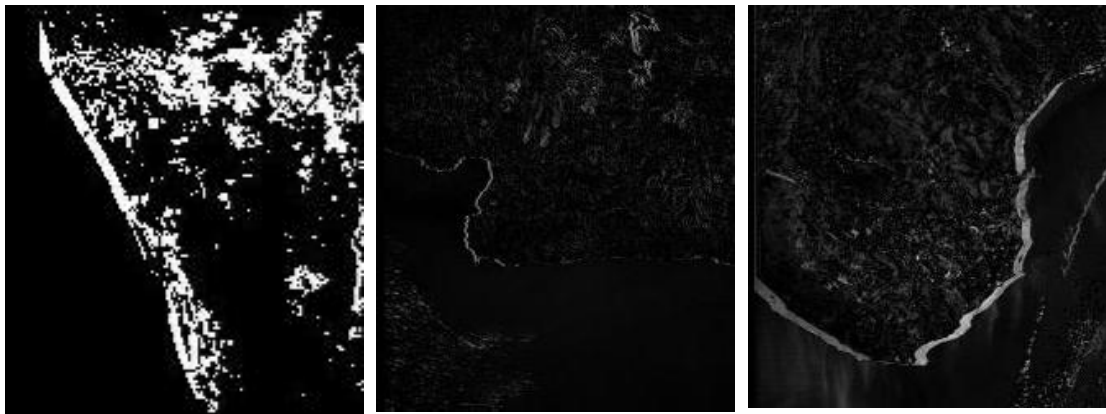


Figure 5.28 Classification Using SVM

So it is possible to quantifiably depict the amount of increase of water body in 2010 when compared to 2005 as shown in Figure 5.29.



Kochi Region

Indonesia Region

Kanyakumari Region

Figure 5.29 Change depicted over five years

Table 5.2 Coverage areas of water body and non-water body of different landscapes in percentage

Area	2005	2005	2010	2010	Changes detected in the period of 5 years
	Water	Non-water	water	Non-water	
Kochi	26.1200	73.88	29.2	70.8	3.08%
Indonesia	46.6476	53.3524	46.6599	53.3401	0.01%
Kanyakumari	46.4966	53.5034	44.2856	55.7144	0.16%
Vishakhapatnam	62.8494	37.1506	63.5956	36.4044	0.74%
Sydney	56.3477	43.6523	60.0342	39.9658	3.68%
Kolkata	27.4445	72.555	31.7780	68.2220	4.333%

5.7.4 Accuracy Calculation

The percentage of changes in water body and non-water body can be interpreted from the results shown in Table 5.2. The count has been materialised by taking pixel values of the classified image into account as the input, and then pixels of the water region are counted first which leads to the count of the non-water body. The change in coverage area of water body has recorded a significant increase over five years in the study region, as shown in Table 5.2. The increase in the coverage areas of water bodies due to global warming has been substantially proven through these results.

5.8 APPLICATION – GLACIER CLASSIFICATION

The advent of global warming and thus the glacier meltdown has been a serious issue amongst the various environmental bodies of the world. The efficient analysis of LANDSAT images can provide valuable results and

information which can help strategize the preventive steps taken by the environmental bodies. The main aim of this is to compare the K-Means and Fuzzy C-Means clustering technique and find out the change detection in glacier classification by processing images taken over different time frames.

The classification of glaciers and determining the percentage of change in glaciers over a time frame can give an accurate idea of the repercussions of global warming and thus strategize environmental protection plans for the future. Usage of unsupervised glacier classification over supervised glacier classification can lead to reduction in manual labor and automation of research.

5.8.1 Data Sets

The LANDSAT images correspond to the Himachal Pradesh region, one dated June 2005 and the other dated June 2010 are taken. The Figure 5.30 and Figure 5.31 depict the input LANDSAT images of Himachal Pradesh region during June 2005 and June 2010.

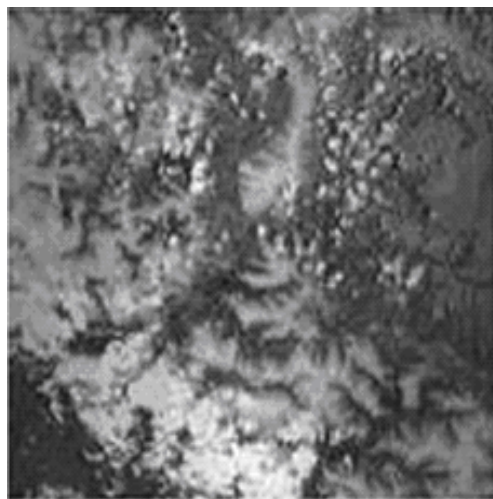


Figure 5.30 June 2005 image of Himachal Pradesh region

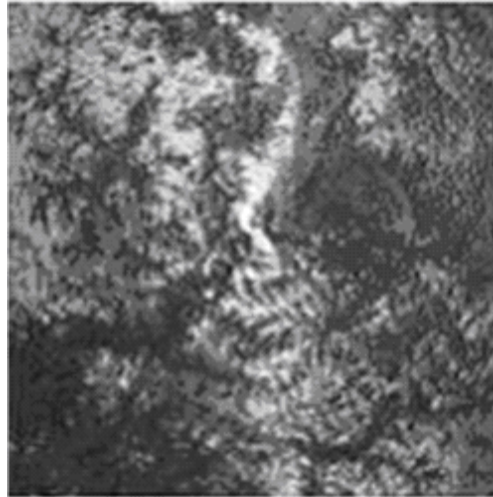


Figure 5.31 June 2010 image of Himachal Pradesh region

5.8.2 Results of K-Means Clustering

The input images have been subjected to K-Means clustering. The Figure 5.32 and Figure 5.33 show the results of K-Means clustering that gives the change of glacier from non-glacier in the given input image. Using the outputs it can be very easy to find out the percentage of change of glacier from non-glacier.

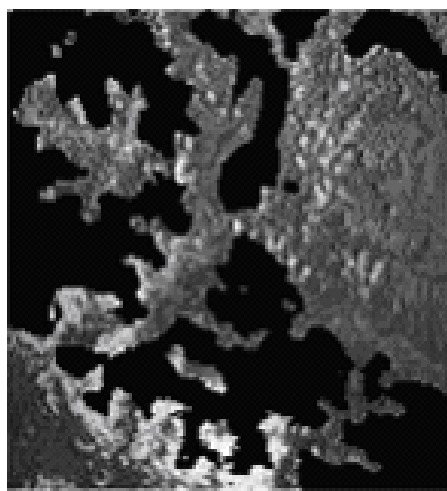


Figure 5.32 Objects identified by K-Means clustering during June 2005

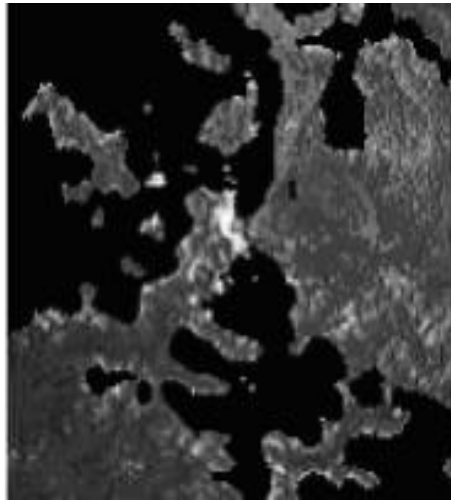


Figure 5.33 Objects identified by K-Means clustering during June 2010

The percentage of glacier and non-glacier in June 2005 image is 36% and 63% and June 2010 is 29% and 71%. So, the change in coverage area of glacier is a significant decrease over five years in the given image by 7% and vice-versa.

5.8.3 Results of Fuzzy C-Means Clustering

The Figure 5.34 and Figure 5.35 portray the results of June 2005 and June 2010 image after applying Fuzzy C-Means clustering. The percentage of change of glacier in June 2005 image over June 2010 image is 8%. In accordance with the real time data, it gives a confidence to indicate that the work to be performed will yield a fruitful result.



Figure 5.34 June 2005 image after applying Fuzzy C-Means clustering

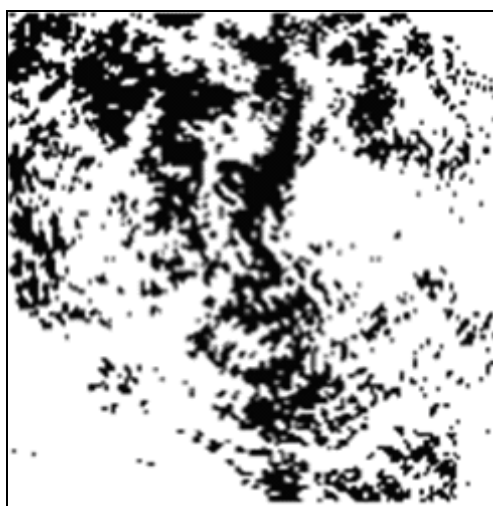


Figure 5.35 June 2010 image after applying Fuzzy C-Means clustering

The glacier classification using the Fuzzy C-Means approach yields a superior result compared to K-Means approach. Using the K-Means approach there are a number of unclassified glacier and so the classification accuracy is low compared to the Fuzzy C-Means approach. According to the ground truth the Fuzzy C-Means clustering derives the better result compared to the K-Means clustering.

5.9 SUMMARY

This chapter explained how the supervised and unsupervised classification techniques are applied for change detection, glacier and water-body classification approaches. The accuracy of the classification techniques are evaluated by receiver operating characteristics. The next chapter provides a comparative study of how all the techniques discussed so far are used for improving classification accuracy.